Subdiffusion equation with Caputo fractional derivative with respect to another function in modeling diffusion in a complex system consisting of a matrix and channels

Tadeusz Kosztołowicz [*]
Institute of Physics, Jan Kochanowski University, Uniwersytecka 7, 25-406 Kielce, Poland

Aldona Dutkiewicz [†]
Faculty of Mathematics and Computer Science, Adam Mickiewicz University, Uniwersytetu Poznańskiego 4, 61-614 Poznań, Poland

Katarzyna D. Lewandowska [‡]
Department of Radiological Informatics and Statistics, Medical University of Gdańsk, Tuwima 15, 80-210 Gdańsk, Poland

Sławomir Wąsik [§]
Department of Medical Physics and Biophysics, Institute of Physics, Jan Kochanowski University, Uniwersytecka 7, 25-406 Kielce, Poland

Michał Arabski [‖]
Institute of Biology, Jan Kochanowski University, Uniwersytecka 7, 25-406 Kielce, Poland

Anomalous diffusion of an antibiotic (colistin) in a system consisting of packed gel (alginate) beads immersed in water is studied experimentally and theoretically. The experimental studies are performed using the interferometric method of measuring concentration profiles of a diffusing substance. We use the *g*-subdiffusion equation with the fractional Caputo time derivative with respect to another function *g* to describe the process. The function *g* and relevant parameters define anomalous diffusion. We show that experimentally measured time evolution of the amount of antibiotic released from the system determines the function *g*. The process can be interpreted as subdiffusion in which the subdiffusion parameter (exponent) α decreases over time. The *g*-subdiffusion equation, which is more general than the "ordinary" fractional subdiffusion equation, can be widely used in various fields of science to model diffusion in a system in which parameters, and even a type of diffusion, evolve over time. We postulate that diffusion in a system composed of channels and a matrix can be described by the *g*-subdiffusion equation, just like diffusion in a system of packed gel beads placed in water.

I. INTRODUCTION

Subdiffusion is a process in which the movement of molecules is very hindered by a complex internal structure of the medium [1–8]. This process was observed, among others, in the diffusion of sugars in agarose gel [9] and in antibiotics diffusion in a bacterial biofilm [10,11]; the reference list can be extended significantly. A distinctive feature of "ordinary" subdiffusion is the relation $\sigma^2(t) \sim t^\alpha$, where σ^2 is the mean square displacement of a diffusing particle and $\alpha \in (0, 1)$. In general, subdiffusion occurs when the time of a molecule to jump is anomalously long. Within the continuous time random walk model, for ordinary subdiffusion the distribution of a waiting time for a molecule to jump ψ has a heavy tail, $\psi(t) \sim$ $1/t^{\alpha+1}$, and the average value of this time is infinite. Ordinary subdiffusion can be described by a differential equation with a time derivative of fractional order controlled by the parameter α [1–8,12].

The situation is more complicated when molecules diffuse in a system consisting of a matrix and channels. The channels are defined here as "free spaces" in the matrix which usually have a complicated geometric structure. The channels can be free spaces in a porous medium, tubules, or spaces between packed beads. Diffusion occurs mainly in channels, but molecules can diffuse into and out of the matrix. The diffusion of various substances in a system consisting of channels and a matrix has been considered in medicine, biology, engineering, geology, agriculture, and other fields of science. Examples include the diffusive release of vitamin from collagen [13], nutrients from a fertilizer to water and sand [14], fertilizers from beads [15,16], diffusion of oxygen in soils [17], the process of active ingredients release which can be used in the reduction of groundwater pesticide pollution [18], insulin release from chitosan beads [19], and drug release from alginate beads [20,21] and from coating beads [22]. Such

———————
[*]tadeusz.kosztolowicz@ujk.edu.pl
[†]szukala@amu.edu.pl
[‡]katarzyna.lewandowska@gumed.edu.pl
[§]s.wasik@ujk.edu.pl
[‖]arabski@ujk.edu.pl

studies are needed to establish the conditions under which the optimal dose of the drug is released [23,24]. Theoretical models of the processes mentioned above have been based on diffusion-reaction equations [17,24–30], the ordinary subdiffusion equation with Caputo derivative in which a source term is involved [31], the ordinary subdiffusion-reaction equation [32], and on the scaling approach [33]. Subdiffusion parameters depend on the disorder of packing beads [34,35] and on the structure of beads [36].

We assume that the process could be described by the ordinary subdiffusion equation with a fixed parameter α at some initial time interval. The normal diffusion equation may be treated as a special case of the ordinary subdiffusion equation for $\alpha = 1$, and thus we do not exclude normal diffusion from further considerations. However, getting the molecules into the beads and back again can slow down the subdiffusion. Similar processes in which the diffusion of molecules is interrupted by their trapping in an immobile zone have been considered in [33,37–39]. Traps can be small caves with narrow passages. Such traps change the timescale of the process [40,41]. To describe the process, we use a subdiffusion equation with the fractional Caputo derivative with respect to another function g [42–44] which controls the slowness of the process. We call this equation the g-subdiffusion equation. The key is to determine the g function experimentally. For this purpose, it is convenient to define a function describing the diffusion process and controlled by the function g that is relatively easy to measurable experimentally.

In the following, we experimentally study the diffusion of an antibiotic (colistin) in a system in which gel (alginate) beads soaked with the antibiotic are placed in water. We use the g-subdiffusion equation to describe the process and show that the time evolution of the amount of the antibiotic released from the system allows the determination of the function g.

II. EXPERIMENT

The system used for the experimental study consists of two regions A ($x < 0$) and B ($x > 0$) separated by a thin membrane located at $x = 0$; see Fig. 1. We assume that the system is homogeneous in the plane perpendicular to the x axis, so it is effectively one dimensional. The membrane, which is very permeable to diffusing particles, keeps the beads in region A. At the initial moment, all of the antibiotic is in beads; it is distributed uniformly in each bead. The antibiotic concentration is measured by means of the interferometric method. Since the region containing the beads is not transparent to the laser beam, measurements of the antibiotic concentration can only be made in region B. We focus our attention on a time evolution of the amount of the antibiotic, $N(t)$, that has diffused from region A to B.

The scheme of the system is shown in Fig. 1. The system consists of two vessels separated by a thin membrane. The vessel sizes are as follows: the cross-sectional area is $S = 7 \times 10^{-5}$ m^2, the length of the vessel A (measured along the x axis) is $L_A = 10^{-2}$ m, and the length of the vessel B is $L_B = 5 \times 10^{-2}$ m. Antibiotic soaked alginate beads were made as follows. 1 mg of colistin in the form of methanesulfonate sodium (Fluka) was dissolved in 1 ml of 1.5% alginate solution. Using an automatic pipette, the alginate solution
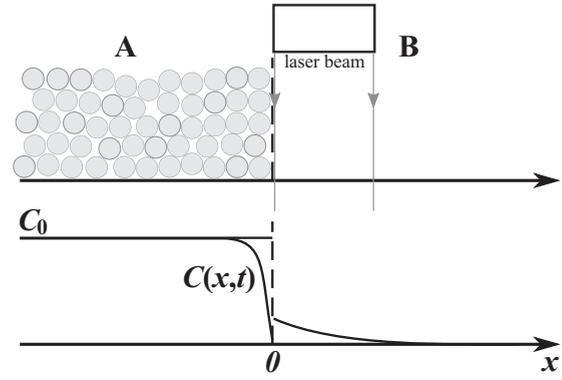

FIG. 1. Top panel: Scheme of the system used in the experiment; region (vessel) A contains alginate beads impregnated with colistin placed in water and region B contains water at the initial moment. As the beads are nontransparent to the laser beam, interferometric measurement of the concentration is only possible in region B. Lower panel: C denotes the concentration of the antibiotic; C_0 is the initial concentration in region A.

with an antibiotic was added dropwise to a calcium chloride solution of 0.15 mol/m^3 concentration. As a hydrogel carrier, the sodium alginate (SAFC) was used. Due to the biocompatibility, as a crosslinking agent, calcium cations were applied, the source of which was calcium chloride (POCH S.A.). A single bead has a volume of 15 μl. 27 beads were in vessel A, and the ratio of the total volume of all beads to the volume of vessel A was equal to 0.58. Within the homogeneous medium approximation, the initial colistin concentration in vessel A was calculated using the formula $\mathcal{C}_0 = \mathcal{N}_0 / V_A$, where $\mathcal{N}_0$ is the total amount of colistin in all beads at the initial moment. We obtained $\mathcal{C}_0 = 0.50$ mol/m^3. The linear initial concentration used in the theoretical model $C_0 = S\mathcal{C}_0$ was $C_0 = 3.5 \times 10^{-5}$ mol/m. Concentration profiles of the antibiotic were determined in region B for different times $t \in [120$ s, 2400 s$]$.

For the experimental study, we used colistin in the form of methanesulfonate sodium (Fluka). Antibiotic solutions were prepared in double deionized water. The hydrogel carrier was sodium alginate (SAFC), and calcium cations were selected as the cross-linking agent due to their biocompatibility. The source of calcium cations was calcium chloride (POCH S.A.). In order to prepare alginate beads with colistin, 1 mg of colistin was dissolved in 1 ml of a 1.5% alginate solution and mixed thoroughly. Then, using an automatic pipette, the alginate-antibiotic solution was dripped into the 0.15 mol/m^3 calcium chloride solution also containing the antibiotic. As a result of gelation, beads having a volume of approximately 15 μl were obtained.

The colistin concentration has been measured by means of the laser interferometric method [9,10,45,46]. Figure 2 presents the sketch of the measuring apparatus. The main element of the apparatus is the double-beam Mach-Zehnder interferometer with a laser illumination system and a computerized system for the recording and processing of interference images. The laser beam produced by a 15 mW He–Ne laser is spatially filtered and, using the beam expander, is then transformed into a parallel beam of width of 80 mm and later split into two beams. One of them passes through both cuvettes
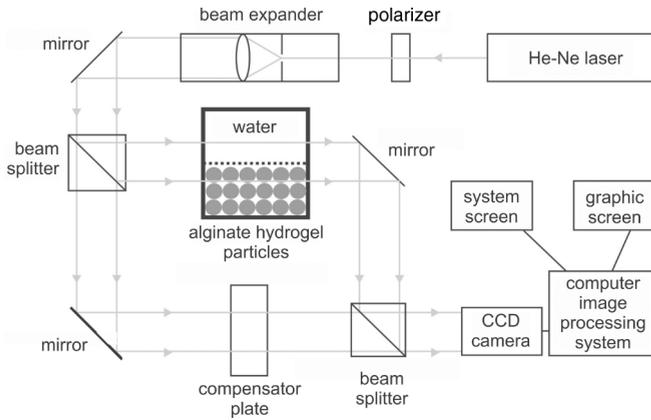
FIG. 2. Experimental setup. Detailed description is in the text.

FIG. 4. Schematic drawing of the interference fringes.

where $\Delta C(x,t) = C_I - C(x,t)$, C_I is the initial concentration,

$$\Delta n(x,t) = \frac{\lambda d(x,t)}{hf}, \qquad (2)$$

where λ denotes a wavelength of the laser light (632.8 nm), h is the distance between the interferometric fringes in the area where they are parallel, and f denotes the thickness of the solution layer along the course of the laser beam. The coefficient a was determined in a separate experiment using the interference refractometer (Zeiss). In the range of tested concentration, the dependence of the refractive index on the concentration of the colistin solution is linear and the value of the parameter a is 2.92×10^3 mol/m^3. The sign of the deviation of the interference fringe d depends on the measurement setup settings. In the experiment, $d(x,t) < 0$ means that in the observed region, the interference fringe deviates to the right and the substance flows in from other regions, which means that the concentration in this region is increasing relative to the initial concentration. When $d(x,t) > 0$, the interference fringe deviates to the left and the substance flows away to the other regions, which means the concentration in this region is decreasing relative to the initial concentration.

The diffusion cell consists of two vessels made of glass with a very high optical homogeneity separated by a horizontally located thin membrane (see Fig. 2). Initially, the alginate beads with colistin of concentration 1 mg/ml were placed close together, completely filling the volume of the lower cuvette, while the upper cuvette was filled with pure water, and thus $C_I = 0$. Then, an antibiotic diffuses to the upper cuvette. The duration of the experiment was 40 min and interferograms were recorded with time interval equal to 2 min. The measurements was conducted under isothermal conditions at a temperature of $T = 295 \pm 0.3$ K.

parallel to the membrane surface, while the other, being a reference beam, goes directly through the compensation plate to the light detecting system where it superimposes with the laser beam which passes through the diffusion cell. The result is the formation of interference fringes; see Fig. 3.

The course of the interference fringes is determined by the refractive index of the solution, which in turn depends on its concentration. Interference fringes are straight when the solute is homogeneous and bend when a concentration gradient is nonzero. The magnitude of the deviation of the interference fringe at a given point with respect to an undisturbed fringe $d(x,t)$ (see Fig. 4) reflects the changes in the refractive index between these points and thus provides information about changes in the concentration of the substance between the points.

The relation between the change of the substance concentration, $\Delta C(x,t)$, and the change of the refractive index, $\Delta n(x,t)$, is linear [47–50],
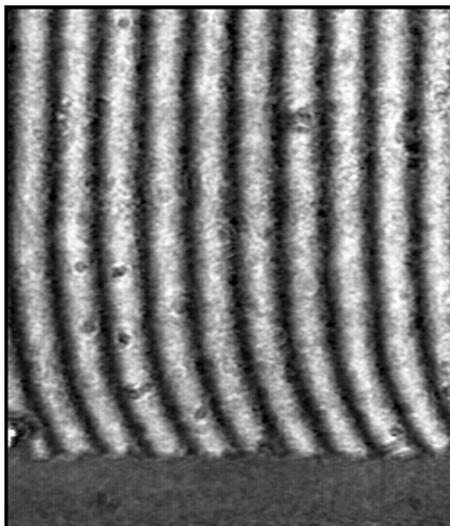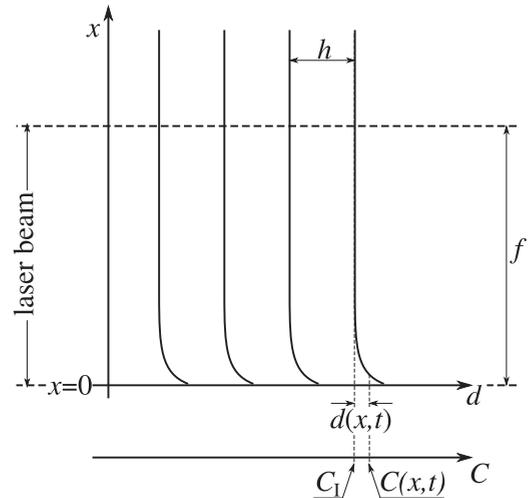
$$\Delta C(x,t) = a\Delta n(x,t), \qquad (1)$$

FIG. 3. Interferogram obtained after 20 min.

III. THEORY

We use the g-subdiffusion equation to model antibiotic diffusion in a system consisting of antibiotic soaked alginate beads densely packed in water. Normal diffusion or subdiffusion may occur in the spaces between the beads. As we have

mentioned, the motivation behind the use of the *g*-subdiffusion equation is that the release of the antibiotic from the gel beads, as well as the possibility of the antibiotic particles repenetrating the beads, can slow down antibiotic diffusion in the system.

Diffusion in region *A* is a combination of two processes: subdiffusion of the antibiotic molecules inside the bead to their exit outside and their further diffusion mainly in a "free space" between the beads. The border between a bead and the free space is not an obstacle for the particles exiting the bead. However, it is an obstacle for the particles trying to reenter the bead because then the particle must hit a pore on the bead surface. We suppose that the return of the antibiotic molecule to a bead is possible when the molecule moves in region *A* and has frequent contact with the bead surfaces. When a molecule diffuses in region *B* near the border with region *A*, the molecule contact with the beads is much less frequent and the molecule is unlikely to return to region *A*. We assume that the boundary between the regions can be regarded as an absorbing wall for molecules located in region *A*. The most often used boundary condition at the absorbing wall is zero concentration of the diffusing substance at the wall. The amount of antibiotic that is in region *B* is equal to the amount of the antibiotic that left region *A* at the same time. Therefore, in the following, we consider diffusion of the antibiotic in region *A*. We use the approximation of a homogeneous medium for region *A* and assume that the medium structure does not change in time. Then, the medium consisting of beads and free spaces between beads has assigned subdiffusion parameters such as for a homogeneous medium; a similar approximation has been used in the modeling of diffusion in a disordered system of spheres [34,35]. We also assume that the parameters are independent of time and a spatial variable and the antibiotic is distributed homogeneously in region *A* at the initial moment. The parameters presented later in this paper and Eq. (8) show that $\sigma \approx 0.036$ cm for $t = 2400$ s, whereas the length of vessel *A* is 1.0 cm. Thus, we suppose that the influence of the outer wall of vessel *A* on molecules diffusing from *A* to *B* is negligibly small; at the outer wall, the concentration is still C_0. To simplify the calculations, we assume that the wall is located at $-\infty$. The diffusion of antibiotic molecules in vessel *A* is described by the *g*-subdiffusion equation (6), the initial condition is $C(x, 0) = C_0$, and the boundary conditions are $C(-\infty, t) = C_0$ and $C(0^-, t) = 0$.

Subdiffusion is often described by the subdiffusion equation with the Riemann-Liouville fractional time derivative [1–4,12], which may be converted to the following form:

$$\frac{^C\partial^\alpha \tilde{C}(x,t)}{\partial t^\alpha} = D\frac{\partial^2 \tilde{C}(x,t)}{\partial x^2}, \tag{3}$$

with the "ordinary" Caputo derivative of the order $\alpha \in (0, 1)$ defined as

$$\frac{^C\partial^\alpha f(t)}{\partial t^\alpha} = \frac{1}{\Gamma(1-\alpha)} \int_0^t (t-u)^{-\alpha} f'(u) du. \tag{4}$$

D is a subdiffusion coefficient given in the units of m²/s$^\alpha$. We call Eq. (3) the "ordinary" subdiffusion equation and its solution is denoted here as $\tilde{C}$. Recently, differential equations with a fractional Caputo derivative with respect to another function *g* (the *g*-Caputo fractional derivative) have been considered

[51–54]. For $\alpha \in (0, 1)$, this derivative is defined as

$$\frac{^C d_g^\alpha f(t)}{dt^\alpha} = \frac{1}{\Gamma(1-\alpha)} \int_0^t [g(t) - g(t')]^{-\alpha} f'(t') dt', \tag{5}$$

and the function *g*, which is given in a time unit, fulfills the conditions $g(0) = 0$, $g(\infty) = \infty$, and $g'(t) > 0$ for $t > 0$. Involving this derivative in the diffusion equation, we get the *g*-subdiffusion equation,

$$\frac{^C\partial_g^\alpha C(x,t)}{\partial t^\alpha} = D\frac{\partial^2 C(x,t)}{\partial x^2}. \tag{6}$$

When $g(t) \equiv t$, we have the ordinary subdiffusion equation. Solutions $\tilde{C}$ of the ordinary subdiffusion equation and *C* of the *g*-subdiffusion equation are related to each other as follows [42,43]:

$$C(x,t) = \tilde{C}(x, g(t)), \tag{7}$$

if the boundary conditions, the initial condition, and the parameters α and *D* are the same for both equations. Thus, the *g*-subdiffusion equation describes the subdiffusion process with changed time variable. If diffusion is described by Eq. (6), then the random walk of a single molecule is characterized by the relation [42]

$$\sigma^2(t) = \frac{2Dg^\alpha(t)}{\Gamma(1+\alpha)}. \tag{8}$$

Choosing the function *g* appropriately, we can obtain different functions σ^2 that have been derived from other models, e.g., $g \sim \ln^\alpha t$ for ultraslow diffusion and $g \sim t^{2/d_w}$ for diffusion on a fractal, where d_w is the fractal dimension of a medium; an overview of σ^2 derived from different models is presented in [8,55].

The key is to find the *g* function on the basis of experimental results. A function providing the function *g* is a time evolution of the total amount of the substance that has diffused from region *A* to *B*,

$$N(t) = \int_{-\infty}^0 [C_0 - C(x,t)] dx; \tag{9}$$

see Fig. 1.

Solutions to the *g*-subdiffusion equation can be obtained by means of the *g*-Laplace transform method. This transform is defined as

$$\mathcal{L}_g[f(t)](s) = \int_0^\infty e^{-sg(t)} f(t) g'(t) dt. \tag{10}$$

It has the following property [51,53]:

$$\mathcal{L}_g\left[\frac{^C d_g^\alpha f(t)}{dt^\alpha}\right](s) = s^\alpha \mathcal{L}_g[f(t)](s) - s^{\alpha-1} f(0), \tag{11}$$

which makes the procedure for solving Eq. (6) similar to the procedure for solving ordinary subdiffusion equation (3) using the ordinary Laplace transform $\mathcal{L}[f(t)](s) = \int_0^\infty \exp(-st) f(t) dt$ [42]. In terms of the *g*-Laplace transform, the *g*-subdiffusion equation is

$$s^\alpha \mathcal{L}_g[C(x,t)](s) - s^{\alpha-1} C_0 = D\frac{\partial^2 \mathcal{L}_g[C(x,t)](s)}{\partial x^2}. \tag{12}$$

The solution to this equation for the boundary conditions $\mathcal{L}_g[C(-\infty, t)](s) = C_0/s$, $\mathcal{L}_g[C(0^-, t)](s) = 0$, and the initial condition $C(x, 0) = C_0$ is

$$\mathcal{L}_g[C(x, t)](s) = \frac{C_0}{s}(1 - e^{\sqrt{s^\alpha/D}x}). \qquad (13)$$

The $\mathcal{L}_g$ transform is related to the ordinary Laplace transform by the formula

$$\mathcal{L}_g[f(t)](s) = \mathcal{L}[f(g^{-1}(t))](s). \qquad (14)$$

This formula is helpful in calculating the inverse g-Laplace transforms [51,53]. From the relation $\mathcal{L}_g[1](s) = 1/s$, the g-Laplace transform of Eq. (9), and Eq. (13), we obtain $\mathcal{L}_g[N(t)](s) = C_0\sqrt{D}/s^{1+\alpha/2}$. Using the formula $\mathcal{L}_g^{-1}[1/s^{1+\beta}](t) = g^\beta(t)/\Gamma(1 + \beta)$, $\beta, s > 0$, we get

$$N(t) = \kappa g^{\alpha/2}(t), \qquad (15)$$

where

$$\kappa = \frac{C_0\sqrt{D}}{\Gamma(1 + \alpha/2)}. \qquad (16)$$

For ordinary subdiffusion, we have

$$N(t) = \kappa t^{\alpha/2}. \qquad (17)$$

The function for normal diffusion is obtained from the above equations putting $\alpha = 1$,

$$N(t) = \frac{2C_0\sqrt{D}}{\sqrt{\pi}}\sqrt{t}. \qquad (18)$$

IV. DETERMINATION OF THE FUNCTION g AND THE PARAMETERS α AND D

We assume that properties of the medium do not change rapidly, and thus the function N is smooth, i.e., its derivative is continuous. Since $N(t) \sim \sigma(t)$, we use N to identify the type of diffusion. When N is a power function with an exponent less than $1/2$, the process can be treated as subdiffusion. The empirical results and the power functions N given by Eq. (17) with $\alpha = 0.5$ (solid line) and Eq. (18) for normal diffusion (dashed line) are presented in the logarithmic scale in Fig. 5. The slope of the lines representing N depends on the parameter α only.

From Fig. 5, we conclude that (1) the process under study is not normal diffusion, (2) the process is not ordinary subdiffusion with constant parameter α over the entire time domain, (3) the process can be treated as ordinary subdiffusion only in some initial time interval (we estimate it as $t \leqslant 480$ s, which corresponds to four initial points in the plot), and (4) for longer times, the process is slower than the ordinary subdiffusion mentioned in point (3).

Based on the above conclusions, we assume that (i) for $t \in [0, 480$ s], the process is ordinary subdiffusion with parameters α and D, (ii) for later times, the process is g subdiffusion with function g, which generates the relation

$$N(t) = \kappa t^{\tilde{\alpha}(t)/2}, \qquad (19)$$

where $\tilde{\alpha}(t)$ fulfills the conditions $0 < \tilde{\alpha}(t) \leqslant 1$ and $\tilde{\alpha}(0) = \alpha$. Equations (15) and (19) provide $g(t) = t^{\tilde{\alpha}(t)/\alpha}$. Parameters α and D in the g-subdiffusion equation (6) are the same as
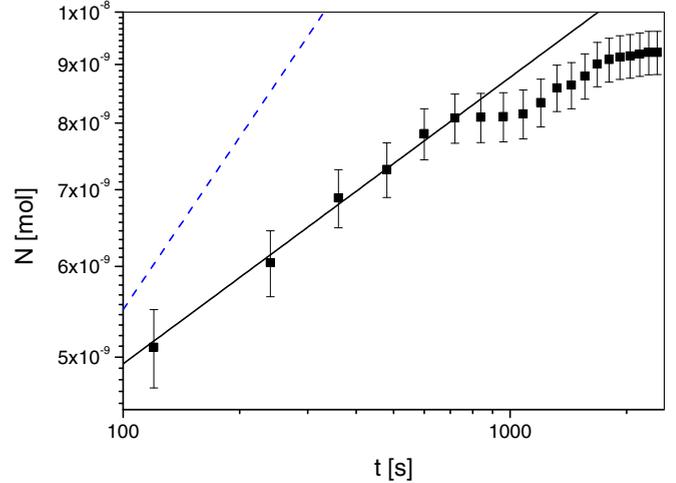

FIG. 5. Plots of the power functions $N(t) = 1.57 \times 10^{-9}t^{0.25}$ for ordinary subdiffusion (solid line) and $N(t) = 0.55 \times 10^{-9}\sqrt{t}$ for normal diffusion (dashed line) in the log-log scale; the empirical results are denoted by symbols. The function for normal diffusion is an example; it does not represent any process considered in this paper.

for the initial ordinary subdiffusion process. Equation (19) is a generalization of Eq. (17) for the case of a time-varying subdiffusion parameter (exponent).

In further considerations, we assume

$$\tilde{\alpha}(t) = \frac{\alpha}{1 + \beta t}, \qquad (20)$$

where β is a parameter measured in the unit of $1/s$. Comparing Eqs. (15) and (19), the latter with the exponent given by Eq. (20), we obtain

$$g(t) = \kappa^{2/\alpha}t^{1/(1+\beta t)}. \qquad (21)$$

Figure 5 shows that for $t \in [120$ s, 480 s], the data are described well by the function N given by Eq. (17) with $\alpha = 0.5$ and $\kappa = 1.57 \times 10^{-9}$ mol/s$^{0.25}$. From the last equation, the value of initial concentration C_0, and Eq. (16), we get $D = 0.58 \times 10^{-9}$ m^2/s$^{0.5}$. Knowing κ and α, we fit the function N given by Eq. (19) with the exponent given by Eq. (20) to the empirical data in the whole time domain; the fit parameter is β only. As shown in Fig. 6, for $\beta = 4.3 \times 10^{-5}$ $1/s$, the fit is good.

V. FINAL REMARKS

We postulate the following: *Diffusion in a system composed of channels and a matrix can be described by the g-subdiffusion equation (6)*, just like diffusion in a system of packed gel beads placed in water. The solution to the g-subdiffusion equation provides the time evolution of the amount of colistin released from region A, which is consistent with the empirical results. We mention that different models of normal and anomalous diffusion, describing the release of substances from the (sub)diffusive medium, give power functions $N(t) \sim t^\beta$ (when ordinary subdiffusion occurs in A) or exponential functions of the form $N(t) \sim 1 - ae^{-bt^\beta}$ in the long-time limit [13,28–30,50,56,57]. In our study, the
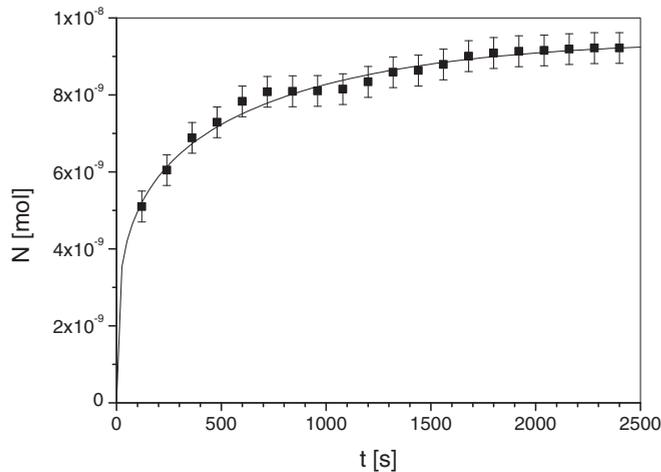
FIG. 6. Plot of the function N given by Eq. (19) with $\tilde{\alpha}(t)$ given by Eq. (20) (solid line) for $\kappa = 1.57 \times 10^{-9}$ mol/s$^{0.25}$, $\alpha = 0.5$, and $\beta = 4.3 \times 10^{-5}$ 1/s; the empirical results are denoted by symbols.

g-subdiffusion equation provides N as a power function with exponent evolving over time. Based on Fig. 5, we conclude that it is not possible to model the diffusion process in region A over the entire time domain using the ordinary subdiffusion equation with a fixed parameter α.

We interpret the fact that the experimentally obtained function N is well approximated by a power function with decreasing subdiffusion parameter $\tilde{\alpha}(t)$ as follows. Colistin (polymyxin E) is a cationic antimicrobial peptide. Due to the presence of five positively charged L-diaminobutyric acid (L-Dab) amino groups in the colistin structure, it is possible that this molecule interacts with calcium alginate. Two mechanisms of polycations binding to alginate have been proposed: an electrostatic interaction and the formation of a calcium alginate gel by displacement of calcium ions in the presence of polycations [58]. Taking into account the interaction of colistin with alginate and the complex geometric structure

of the channels in the alginate gel, subdiffusion of colistin in alginate beads is expected. The first stage of the process is the subdiffusive release of molecules located in the beads close to their surfaces to the space between the beads. This process is ruled by distribution of the waiting time to take the particle next step with a heavy tail controlled by the parameter α, as for ordinary subdiffusion. Initially, releasing antibiotic molecules from region A to B is subdiffusion of the molecules from the beads located at the border between the regions. Later, the process may change its nature when molecules located in A in the layers more distant from the border diffuse into region B. These molecules have a more complicated path from the inside of vessel A to vessel B.

The g-subdiffusion equation offers greater possibilities for modeling subdiffusion processes compared to the ordinary subdiffusion equation. Recently, anomalous diffusion equations with various fractional derivatives have been considered; see the references cited in Ref. [42]. Unfortunately, such equations often do not have a stochastic interpretation. The interpretation of Eq. (6) is based on Eq. (7). We mention that the derivation of Eq. (6) can be based on the ordinary continuous time random walk model [1,2], in which, as in Eq. (7), the time variable in the distribution of waiting time for a molecule to jump is changed, $\psi(t) \to \psi(g(t))$ [43].

The model of diffusion in a matrix with channels system can be used, among others, in the mathematical characteristic of a drug delivery system for wound healing [59], the extracellular matrix mimetic to deliver and retain therapeutic cells at the site of administration for tissue engineering and regenerative medicine [60,61], or "smart" hydrogels as thermo- or pH-responsive [62]. Alginate and the other polysaccharides are the most commonly used materials for polymyxin delivery systems as they provide suitable drug loading efficiency and controlled drug release. So, it seems to be important to characterize these effects on a theoretical level for proper design of the chemical structure of gels as a controlled matrix for drug release. It is crucial for effective bacteria eradication by a lethal concentration of antibiotics obtain in the wound healing environment or stimuli for tissue regeneration [63].

[1] R. Metzler and J. Klafter, The random walk's guide to anomalous diffusion: A fractional dynamics approach, Phys. Rep. **339**, 1 (2000).

[2] J. Klafter and I. M. Sokolov, *First Step in Random Walks. From Tools to Applications* (Oxford University Press, New York, 2011).

[3] E. Barkai, R. Metzler, and J. Klafter, From continuous time random walks to the fractional Fokker-Planck equation, Phys. Rev. E **61**, 132 (2000).

[4] E. Barkai, Fractional Fokker-Planck equation, solution, and application, Phys. Rev. E **63**, 046118 (2001).

[5] A. G. Cherstvy, S. Thapa, C. E. Wagner, and R. Metzler, Non-Gaussian, non-ergodic, and non-Fickian diffusion of tracers in mucin hydrogels, Soft Matter **15**, 2526 (2019).

[6] A. V. Chechkin, J. Klafter, and I. M. Sokolov, Fractional Fokker-Planck equation for ultraslow kinetics, Europhys. Lett. **63**, 326 (2003).

[7] S. I. Denisov and H. Kantz, Continuous-time random walk with a superheavy-tailed distribution of waiting times, Phys. Rev. E **83**, 041132 (2011).

[8] R. Metzler, J-H. Jeon, A. G. Cherstvy, and E. Barkai, Anomalous diffusion models and their properties: non-stationarity, non-ergodicity, and ageing at the centenary of single particle tracking, Phys. Chem. Chem. Phys. **16**, 24128 (2014).

[9] T. Kosztołowicz, K. Dworecki, and S. Mrówczyński, How to Measure Subdiffusion Parameters, Phys. Rev. Lett. **94**, 170602 (2005).

[10] T. Kosztołowicz, R. Metzler, S. Wąsik, and M. Arabski, Modelling experimentally measured of ciprofloxacin antibiotic diffusion in *Pseudomonas aeruginosa* biofilm formed in artificial sputum medium, PLoS One **15**, e0243003 (2020).

[11] T. Kosztołowicz and R. Metzler, Diffusion of antibiotics through a biofilm in the presence of diffusion and absorption barriers, Phys. Rev. E **102**, 032408 (2020).

[12] A. Compte, Stochastic foundations of fractional dynamics, Phys. Rev. E **53**, 4191 (1996).

[13] S. Teimouri, C. Dekiwadia, and S. Kasapis, Decoupling diffusion and macromolecular relaxation in the release of vitamin B6 from genipin-crosslinked whey protein networks, Food Chem. **346**, 128886 (2021).

[14] Ch.-W. Du, J.-M. Zhou, and A. Shaviv, Release characteristics of nutrients from polymer-coated compound controlled release fertilizers, J. Polyn. Environ. **14**, 223 (2006).

[15] S. Fertahi, M. Ilsouk, Y. Zeroual, A. Oukarroum, and A. Barakat, Recent trends in organic coating based on biopolymers and biomass for controlled and slow release fertilizers, J. Control. Release **330**, 341 (2021).

[16] R. Bortoletto-Santos, F. Plotegher, V. F. Majaron, M. G. da Silva, W. L. Polito, and C. Ribeiro, Appl. Clay Sci. **199**, 105874 (2020).

[17] J. Neira, M. Ortiz, L. Morales, and E. Acevedo, Oxygen diffusion in solids: Understanding the factors and processes needed for modeling, Chilean J. Agric. Res. **75**, 35 (2015).

[18] M. Paradelo, D. Soto-Gomez, P. Perez-Rodriguez, E. Pose-Juan, and E. Lopez-Perdiago, Predicting release and transport of pesticides from a granular formulation during unsaturated diffusion in porous media, J. Contam. Hydrol. **158**, 14 (2014).

[19] S. Jose, J. F. Fangueiro, J. Smitha, T. A. Cinu, A. J. Chacko, K. Premaletha, and E. B. Souto, Predictive modeling of insulin release profile from cross-linked chitosan microspheres, Eur. J. Med. Chem. **60**, 249 (2013).

[20] R. M. Iskakov, A. Kikuchi, and T. Okano, Time-programmed pulsality release of dextran from calcium-alginate gel beads coated with carboxy-n-propylacrylamide copolymers, J. Control. Release **80**, 57 (2002).

[21] X. Yuan, R. Liu, W. Zhang, X. Song, L. Xu, Y. Zhao, L. Shang, and J. Zhang, Preparation of carboxylmethylchitosan and alginate blend membrane for diffusion-controlled release of diclofenac diethylamine, J. Materials Sci. Technol. **63**, 210 (2021).

[22] R. Łunio, W. Sawicki, P. Skoczeń, O. Walentynowicz, and J. Kubasik-Juraniec, Compressibility of gastroretentive pellets coated with Eudragit NE using a single-stroke and a rotary tablet press, Pharm. Develop. Technol. **13**, 323 (2008).

[23] I. C. Macha, B. Ben-Nissan, E. N. Vilchevskaya, A. S. Morozowa, B. Emek Abali, W. H. Muller, and W. Rickert, Drug delivery from polymer-based nanopharmaceuticals–An experimental study complemented by simulations of selected diffusion processes, Front. Bioeng. Biotechnol. **7**, 37 (2019).

[24] Y. Fu and W. J. Kao, Drug release kinetics and transport mechanisms of non-degradable and degradable polymeric delivery systems, Expert Opin. Drug Deliv. **7**, 429 (2010).

[25] L. Liu, I. Neretnieks, P. Shahkarami, S. Meng, and L. Moreno, Solute transport along a single fracture in a porous rock: A simple analytical solution and its extension for modeling velocity dispersion, Hydrogeol. J. **26**, 297 (2018).

[26] N. Ray, T. van Noorden, F. Radu, W. Friess, and P. Knabner, Drug release from collagen matrices including an evolving microstructure, Z. Angew. Math. Mech. **93**, 811 (2013).

[27] J. R. Weiser and W. M. Saltzman, Controlled release for local delivery of drugs: Barriers and models, J. Control. Release **190**, 664 (2014).

[28] C. Mircioiu, V. Voicu, V. Anuta, A. Tudose, C. Celia, D. Paolino, M. Fresta, R. Sandulovici, and I. Mircioiu, Mathematical modeling of release kinetics from supramolecular drug delivery system, Pharmaceutics **11**, 140 (2019).

[29] N. A. Peppas and B. Narasimhan, Mathematical models in drug delivery: How modeling has shaped the way we design new drug delivery systems, J. Control. Release **190**, 75 (2014).

[30] J. Siepmann and F. Siepmann, Modeling of diffusion controlled drug delivery, J. Control. Release **161**, 351 (2012).

[31] A. Chang, H. Sun, C. Zhang, B. Lu, C. Lu, R. Ma, and Y. Zhang, A time fractional convection-diffusion equation to model gas transport through heterogeneous soil and gas reservoirs, Physica A **502**, 356 (2018).

[32] E. K. Lenzi, M. A. F. dos Santos, M. K. Lenzi, D. S. Vieira, and L. R. da Silva, Solutions for a fractional diffusion equation: Anomalous diffusion and adsorption-desorption processes, J. King Saud University - Science **28**, 3 (2016).

[33] C. Olivares and F. D. A. Aarão Reis, Interplay of adsorption and surface mobility in tracer diffusion in porous media, Phys. Rev. E **100**, 022120 (2019).

[34] D. Hlushkou and U. Tallarek, Analysis of microstructure-effective diffusivity relationships for the interparticle pore space in physically reconstructed packed beds, J. Chromatogr., A **1581–1582**, 173 (2018).

[35] M. Palombo, A. Gabrielli, V. D. P. Servedio, G. Ruocco, and S. Capuani, Structural disorder and anomalous diffusion in random packing of spheres, Sci. Rep. **3**, 2631 (2013).

[36] M. V. Tamm, L. I. Nazarov, A. A. Gavrilov, and A. V. Chertovich, Anomalous Diffusion in Fractal Globules, Phys. Rev. Lett. **114**, 178102 (2015).

[37] T. J. Doerries, A. V. Chechkin, R. Schumer, and R. Metzler, Rate equations, spatial moments, and concentration profiles for mobile-immobile models with power–law and mixed waiting time distributions, Phys. Rev. E **105**, 014105 (2022).

[38] B. Ling, C. B. Rizzo, I. Battiato, and F. P. J. de Barros, Macroscale transport in channel-matrix system via integral transforms, Phys. Rev. Fluids **6**, 044501 (2021).

[39] O. Bénichou, N. Meunier, S. Redner, and R. Voituriez, Non-Gaussianity and dynamical trapping in locally activated random walks, Phys. Rev. E **85**, 021137 (2012).

[40] D. Holcman and Z. Schuss, Time scale of diffusion in molecular and cellular biology, J. Phys. A: Math. Theor. **47**, 173001 (2014).

[41] D. Holcman and Z. Schuss, Control of flux by narrow passages and hidden targets in cellular biology, Rep. Prog. Phys. **76**, 074601 (2013).

[42] T. Kosztołowicz and A. Dutkiewicz, Subdiffusion equation with Caputo fractional derivative with respect to another function, Phys. Rev. E **104**, 014118 (2021).

[43] T. Kosztołowicz and A. Dutkiewicz, Stochastic interpretation of g-subdiffusion process, Phys. Rev. E **104**, L042101 (2021).

[44] T. Kosztołowicz, First-passage time for the g-subdiffusion process of vanishing particles, Phys. Rev. E **106**, L022104 (2022).

[45] S. Wąsik, M. Arabski, K. Dworecki, J. Janoska, J. Semaniak, K. Szary, and A. Ślęzak, Laser interferometric analysis of glucose and sucrose diffusion in agarose gel, Gen. Physiol. Biophys. **33**, 383 (2017).

[46] T. Kosztołowicz, S. Wąsik, and K. D. Lewandowska, How to determine a boundary condition for diffusion at a thin membrane from experimental data, Phys. Rev. E **96**, 010101(R) (2017).

[47] Y.-L. Yeh, Real-time measurement of glucose concentration and average refractive index using a laser interferometer, Opt. Lasers Eng. **46**, 666 (2008).

[48] J. F. Torres, A. Komiya, E. Shoji, J. Okajima, and S. Maruyama, Development of phase-shifting interferometry for measurement of isothermal diffusion coefficients in binary solutions, Opt. Lasers Eng. **50**, 1287 (2012).

[49] B. Yuan, W. Lt, C. Wang, and L. Li, Sensing of the dynamic concentration field at the solid/liquid interface using a Mach-Zehnder interferometer, Sens. Actuators B **176**, 509 (2013).

[50] B. Yuan, S. Chen, X. Yang, C. Wang, and L. Li, Mapping the transient concentration field within the diffusion layer by use of the digital holographic reconstruction, Electrochem. Commun. **10**, 392 (2008).

[51] H. M. Fahad, M. ur Rehman, and A. Fernandez, On Laplace transforms with respect to functions and their applications to fractional diffusion equations, Math. Meth. Appl. Sci., 1 (2021).

[52] R. Almeida, A Caputo fractional derivative of a function with respect to another function, Commun. Nonlinear Sci. Numer. Simulat. **44**, 460 (2017).

[53] F. Jarad and T. Abdeljawad, Generalized fractional derivatives and Laplace transform, Discr. Contin. Dynam. Sys. Ser. S **13**, 709 (2020).

[54] F. Jarad, T. Abdeljawad, S. Rashid, and Z. Hammouch, More properties of the proportional fractional integrals and derivatives of a function with respect to another function, Adv. Diff. Eq. **2020**, 303 (2020).

[55] A. G. Cherstvy, H. Safdari, and R. Metzler, Anomalous diffusion, nonergodicity, and ageing for exponentially and logarithmically time–dependent diffusivity: striking differences for massive versus maschless particles, J. Phys. D: Appl. Phys. **54**, 195401 (2021).

[56] T. Kosztołowicz, Subdiffusion in a system consisting of two different media separated by a thin membrane, Intl. J. Heat Mass Transf. **111**, 1322 (2017).

[57] T. Kosztołowicz, Model of anomalous diffusion-absorption process in a system consisting of two different media separated by a thin membrane, Phys. Rev. E **99**, 022127 (2019).

[58] B. Thu, P. Bruheim, T. Espevik, O. Smidsrød, P. Soon-Shiong, and G. Skjåk, Alginate polycation microcapsules I. Interaction between alginate and polycation, Biomaterials **17**, 1031 (1996).

[59] N. R. Johnson and Y. Wang, Drug delivery systems for wound healing, Curr. Pharm. Biotechnol. **16**, 621 (2015).

[60] G. D. Prestwich and K. E. Healy, Why regenerative medicine needs an extracellular matrix, Expert Opin. Biol. Ther. **15**, 3 (2015).

[61] G. S. Hussey, J. L. Dziki, and S. F. Badylak, Extracellular matrix-based materials for regenerative medicine, Nat. Rev. Mater. **3**, 159 (2018).

[62] N. N. Ferreira, L. M. B. Ferreira, V. M. O. Cardoso, F. I. Boni, A. I. R. Souza, and M. P. D. Gremiao, Eur. Polymer J. **99**, 117 (2018).

[63] N. V. Dubashynskaya and Y. A. Skorik, Polymyxin delivery systems: Recent advances and challenges, Pharmaceuticals **13**, 83 (2020).